

Tight LMC massive star clusters R 127 and R 128[★]

M. Heydari-Malayeri¹, F. Meynadier¹, and N. R. Walborn²

¹ LERMA, Observatoire de Paris, 61 avenue de l'Observatoire, 75014 Paris, France

² Space Telescope Science Institute, 3700 San Martin Drive, Baltimore, Maryland 21218, USA

Received 12 November 2002 / Accepted 7 January 2003

Abstract. We study the Large Magellanic Cloud (LMC) star clusters R 127 and R 128 using imaging and spectroscopy obtained at the ESO NTT telescope. An advanced image restoration technique allows us to resolve these two clusters into at least 14 and 33 stars respectively and obtain their photometry. In particular, we show that the core of R 127 is composed of at least four stars and identify the Luminous Blue Variable (LBV) component. The closest neighbor of the LBV (star #8) is 1'5 away. Moreover, from medium dispersion spectroscopy we determine the spectral types for 19 stars in and near both clusters, and in particular present the first spatially resolved observation of the second brightest component of the R 127 cluster (star #3) situated 3'3 from the LBV. By comparing with evolutionary models we also look into the stellar ages. The oldest stars of the cluster are ~6–8 Myr old, whereas the most massive star of the region (#7), formed ~3 Myr ago as an 80 M_{\odot} star, has turned into an LBV, the “R 127” star.

Key words. stars: early-type – ISM: individual objects: R 127, R 128 – galaxies: Magellanic Clouds

1. Introduction

R 127 and R 128 (Feast et al. 1960) are two Large Magellanic Cloud (LMC) massive stars situated some 300 pc south of the famous 30 Doradus star-forming factory and 150 pc west of the H II region N158 (Henize 1956). They are in fact the brightest members of the two adjacent tight clusters forming NGC 2055 towards the center of the OB association LH 94 (Lucke & Hodge 1970). Although they lie in the H II region DEM 248 (Davies et al. 1976), they are not apparently linked to any specific nebulosity.

R 127, also called Sk-69°220 (Sanduleak 1970) or HDE 269858, is recognized as a Luminous Blue Variable (LBV), a very rare class of evolved massive stars. Parker (1997) listed 8 members in the LMC, while van Genderen (2001) increased the number of members and candidates to 21. In the past they were called S Dor variables, a designation introduced by Kukarkin et al. (1974), and there is a strong tendency by some workers to use the original name. These most luminous stars ($\log L/L_{\odot} \sim 5.0\text{--}6.3$) are characterized by irregular photometric and spectral variations over decades and evolve from a hot (OB-type) visual minimum phase to a cooler (A-type), visual maximum (Humphreys & Davidson 1994). In the Hertzsprung-Russell (H-R) diagram they are located very close to the observed upper luminosity boundary for very

massive stars, the Humphreys-Davidson limit. LBVs are characterized by extreme instability, dramatic outbursts and high mass loss. Between violent eruptions LBVs still lose mass at high rates, 10^{-5} to $10^{-4} M_{\odot} \text{ yr}^{-1}$ (Lamers et al. 2001 and references therein). The material ejected (up to several M_{\odot}) forms a nebula around LBVs with typical sizes of 0.5–2 pc (Nota & Clampin 1997). The properties of LBVs are reviewed by Humphreys & Davidson (1994) and more recently in the proceedings of a special workshop edited by Nota & Lamers (1997). LBVs are believed to be the precursors of Wolf-Rayet stars; however their precise evolutionary state is still poorly understood. R 127 is quite noteworthy even among this small population; it is the brightest LBV star in the LMC ($M_{\text{bol}} = -10.5$ mag) and has the largest magnitude variation ($\Delta V \sim 2.5$ mag) (Stahl et al. 1983; Humphreys & Davidson 1994; van Genderen 2001). Due to its exceptional characteristics, R 127 has been the subject of much research in the past. R 127 was classified as OIafpe extr or WN 9-10 by (Walborn 1977, 1982). A brightening of 0.75 mag later caused its classification as an S Dor variable (Stahl et al. 1983). It was then included in the Long-Term Photometry of Variables organized by Sterken (1983), and published in several papers (Manfroid et al. 1991; Manfroid et al. 1994; Sterken et al. 1993, 1995; van Genderen et al. 1997). The monitoring showed that R 127 had a very bright phase around the end of 1986 with $y = 9.05$ mag, and as such was the brightest star in the LMC (Wolf et al. 1988), only surpassed in February 1987 by SN1987A. R 127 reached its visual maximum of $V \sim 8.8$ mag around the year 1989 and then slowly decreased to $V \sim 9.4$ mag in ~1995.

Send offprint requests to: F. Meynadier,
e-mail: Frederic.Meynadier@obspm.fr

[★] Based on observations obtained at the European Southern Observatory, La Silla, Chile.

A new maximum of $V \sim 9.3$ mag was attained in 1997 coinciding with the time of present observations. Subsequently it became fainter, with $V \sim 10.4$ mag, around the year 2000 (Stahl 2002, private communication).

Infra-red observations have shown that R 127 is surrounded by a dust shell (Stahl et al. 1984). As this dust shell is believed to be a crucial element for understanding the evolution of massive stars, it has been extensively studied using imagery (Stahl 1987), coronagraphy (Clampin et al. 1993), spectroscopy (Smith et al. 1998), and polarimetry (Schulte-Ladbeck et al. 1993).

R 128, otherwise Sk-69°221 or HDE 269859, is a supergiant B2 Ia (Fitzpatrick 1991). It is variable with a total range of 0.32 mag between 1983 and 1990, which is very large for its spectral type (van Genderen et al. 1998). Interestingly, this star has formerly been considered as an LBV candidate (van Genderen 2001).

The studies so far devoted to these two interesting bright stars have mainly dealt with their individual characteristics. However, recent findings, from both high-resolution observations and theoretical works, suggest that massive stars form in groups. Therefore, knowing the characteristics of the cluster members is necessary for better understanding the formation and evolution of these brightest, probably the most massive, stars of the group. Nota et al. (1991) looked into the multiplicity of R 127 by obtaining high-resolution, ground-based images with the STScI coronagraph and reported the presence of 20 stars towards R 127. Although these components are mainly field stars detached from R 127 proper, they detect a relatively close component lying $3''.5$ north-west of the bulk of R 127.

The present work is therefore devoted to the photometry and spectroscopy of the cluster members. Using high resolution imaging techniques, we aim at resolving the cores of the clusters R 127 and R 128. Moreover, high spatial resolution spectroscopy will allow us to study the physical properties of so far unknown members of these two tight clusters.

2. Observations and data reduction

2.1. Sub-arcsecond imaging and deconvolution photometry

The R 127 and R 128 clusters were observed on 20 November 1997 using the ESO New Technology Telescope (NTT) equipped with the active optics SUPERB Seeing Imager (SUSI). The detector was a Tektronix CCD (#42) with 1024×1024 pixels of $24 \mu\text{m}$ ($0''.13$ on the sky), and the seeing varied between $0''.81$ and $1''.34$ (FWHM).

The observations were performed in the *uvby* Strömgren photometric system using the ESO filters # 715, 716, 713, and 714 respectively. We were particularly careful to keep most of the brightest stars in the field under the detector's saturation level to have at our disposal high quality Point Spread Function (PSF) stars. This led us to adopt exposure times of 350, 175, 210 and 140 seconds in *u*, *v*, *b* and *y* respectively. We also used ditherings of $5''$ – $10''$ for bad pixel rejection and in order to be able to use the full oversampling capabilities of the MCS deconvolution algorithm (Magain et al. 1998). Indeed when

performing simultaneous deconvolution of several frames, the algorithm uses the different frame centerings as a constraint while decreasing the pixel size. We took a grid of seven dithering positions for each filter. Luckily, the targets of interest are close enough to be contained in a single SUSI field of view. Unfortunately, the *u* images could not be used for the photometry due to their insufficient quality.

Photometry was derived in the Strömgren *v*, *b* and *y* filters according to the following procedure: after bias subtraction and flat-fielding, the seven frames were co-added in each of the filters. The photometry of the stars lying outside the compact clusters was performed on the resulting frames through the DAOPHOT reduction package. This yielded the photometry of 233 stars situated outside clusters R 127 and R 128 (Fig. 1).

The crowded clusters were processed with the MCS restoration algorithm. The deconvolution was performed on a 256×256 pixel region containing both R 127 and R 128. The MCS code, proposed and implemented by Magain et al. (1998), results from a new approach to deconvolution taking care not to violate the Shannon (1949) sampling theorem: the images are deliberately not deconvolved with the observed PSF, but with a narrower function, chosen so that the final deconvolved image can be properly sampled, whatever sampling step is adopted to represent the final data. For this purpose, one chooses the final, well-sampled PSF of the deconvolved image and computes the PSF which should be used to perform the deconvolution. The observed PSF is constructed from several stars close enough to the clusters in order to avoid any possible PSF variation across the field.

The restoration resolves the R 127 and R 128 clusters into 14 and 33 components respectively (Fig. 2). The deconvolution method requires a high S/N ratio for the sources in order to achieve accurate photometry and astrometry. Therefore, very faint stars too close to the bright components were excluded from the deconvolution process. Star #13 was detected but its magnitude could not be accurately measured, due to the presence of relatively strong process residuals.

A technical problem during the observing run prevented us from obtaining adequate standard star observations necessary for calibrating the photometry. The available calibration frames allowed us however to correct for the atmospheric extinction for all filters and derive the zero point for the *y* filter. Results concerning *y* magnitudes were checked using the photometric data available in the literature for three stars in the field, Sk-69°217, Sk-69°218 and R 128 (Ardeberg et al. 1972; Isserstedt 1975). Intrinsic $(b-y)_0$ colors were calculated for each star of known spectral type (see Sect. 4), in two steps: first we established their effective temperatures from the calibration by Vacca et al. (1996), then the corresponding theoretical $(b-y)_0$ colors were deduced using Relyea & Kurucz (1978). An average interstellar reddening of $E(B-V) = 0.15$ mag (St-Louis et al. 1997), or $E(b-y) = 0.12$ mag (Kaltcheva & Georgiev 1992), was used to obtain the observational $(b-y)$ colors.

The final photometric results for the two clusters R 127, R 128, and the brightest field stars are presented in Tables 1–3 which also list the α - δ (2000.0) positions of the stars. The astrometry was obtained from the identification of several bright,

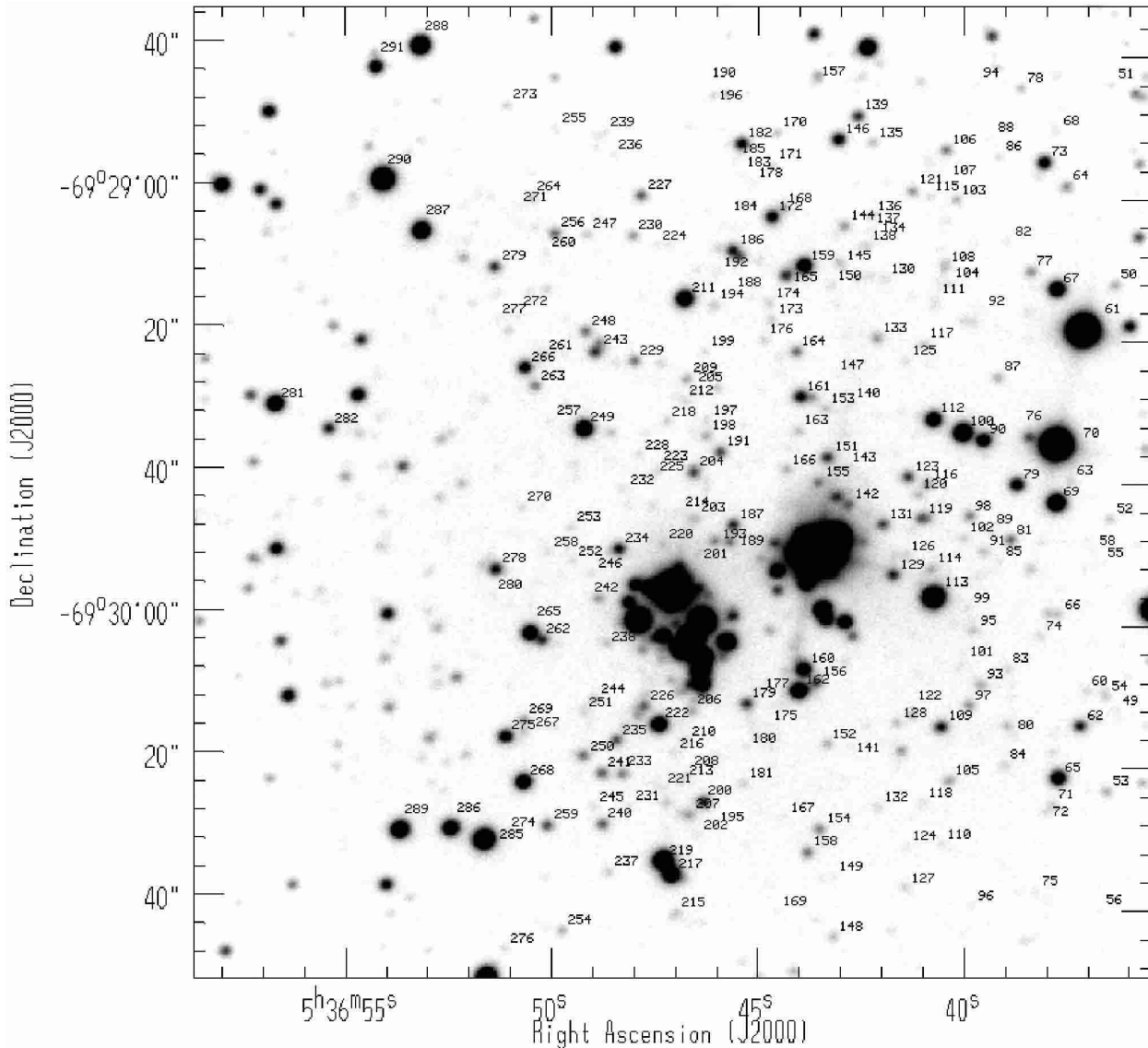


Fig. 1. The LMC star clusters R 127 and R 128 as seen through the Strömgren v filter. The image is based on co-adding 7 dithered individual exposures. R 127 is the cluster lying to the right of the image center. The field size is $2' \times 2'$, corresponding to $31 \text{ pc} \times 31 \text{ pc}$. North is up and east to the left.

isolated stars with GSC 2.2 stars. The positional accuracy is found to be around $2''$.

A word of caution seems appropriate regarding the colors. The powerful deconvolution method has allowed us to resolve the compact clusters R 127 and R 128 revealing their so far unknown components. Furthermore, the code has enabled us to perform the photometry of the tight components. However, we should underline that this photometry is relative for a number of reasons which have nothing to do with the limitations of the code. The shortcomings in the observation of standard photometric stars particularly affect the colors, and we have therefore taken care not to over-interpret them.

2.2. Spectroscopy with NTT/EMMI

The EMMI spectrograph attached to the ESO NTT telescope was used on 22 November 1997 (BLMD mode) to obtain

several long slit spectra. The grating was #12 centered on 4350 \AA and the detector was a Tektronix CCD (#31) with 1024^2 pixels of size $24 \mu\text{m}$. The range was $3810\text{--}4740 \text{ \AA}$ and the dispersion 38 \AA mm^{-1} , giving fwhm resolutions of 2.70 ± 0.10 pixels or $2.48 \pm 0.13 \text{ \AA}$ for a $1''$ slit. At each position we first took a short 5 min exposure followed by one or two longer 15 min exposures. The instrument response was derived thanks to observation of the calibration stars LTT 1020, LTT 1788, EG 21.

The seeing varied from $0''.45$ to $0''.53$, allowing us to obtain uncontaminated spectra. The identification of the stars along the slits was based on sketches drawn during the observations. Since the targets lie in crowded regions, some ambiguous identifications required the development of a small IRAF task, using the position angle information in the FITS headers. First, each spectrum was integrated along the dispersion axis, the result being stored into a two-pixel wide strip, which is close

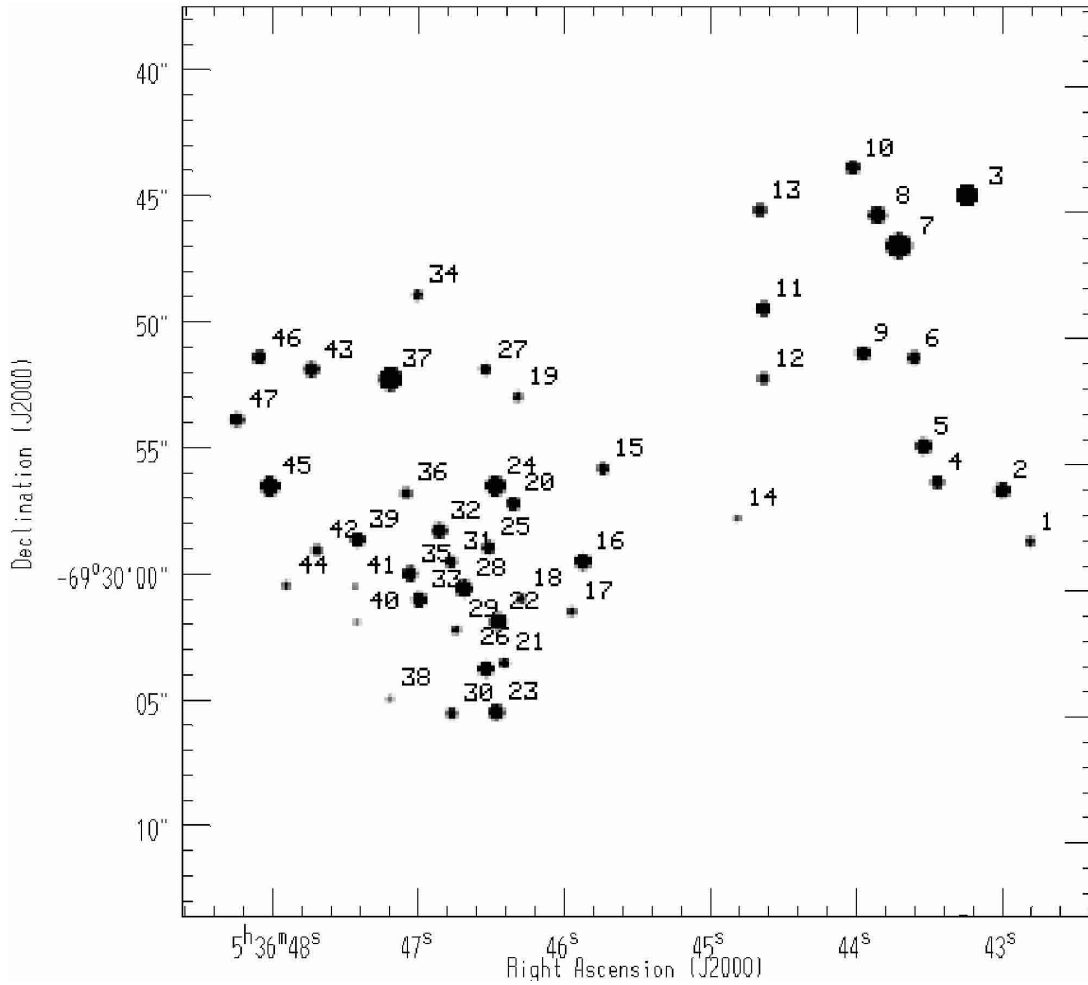


Fig. 2. Restored Strömgren y image of the clusters R 127 and R 128 using the MCS deconvolution method. Star #7 is the main component of the R 127 cluster, resolved into 14 components. R 128 is shown to be made of at least 33 components. Stars outside the clusters were masked during the deconvolution process. The field size is $33''.3 \times 33''.3$ ($8.3 \text{ pc} \times 8.3 \text{ pc}$). North is up and east to the left.

to the actual size of the slit. Then, the position angle and the pixel-arcsec correspondence were used to calculate the rotation matrix for the World Coordinate System. This allowed creation of a slit chart, an α - δ calibrated two-dimensional image containing accurate slit orientations. Displaying simultaneously the slit chart besides the SUSI images and using the WCS correlations it was possible to accurately check the identity of the star in the slit.

3. Photometry results

3.1. Components of the clusters

Figure 1 presents the two tight clusters R 127 and R 128 and their immediately surrounding field (Sect. 3.2). The central image restored by deconvolution is displayed in Fig. 2, while Tables 1–3 list the results of the photometry.

We show that R 127 is composed of at least 14 stars. The brightest component, #7 with $y = 9.37$ and $(b - y) = 0.23$ mag, must be the real LBV (Sect. 4.1). The closest components to #7, stars #8 and #3 having $y = 14.39$ and 12.12 mag respectively, lie at $1''.5$ and $3''.3$ from the main component. Star #3 turns out to be very interesting as shown by its spectrum (Fig. 7). R 127 was the target of coronagraphic imaging through a broad-band

R filter and also a narrow-band $H\alpha + N II$ filter by Clampin et al. (1993) and Nota et al. (1991). They detect star #3 which they call R 127B. Those observations also show the presence of a faint bipolar nebulosity that fails to appear on our frames. On the other hand, their use of a $2''.7$ -diameter masking disk centered on R 127 forbids any detection of the companion identified as star #8. Even star #10 remains undetected, possibly due to low S/N ratio. The existence of stars #8 and #10 is however confirmed by an unpublished R frame which we obtained in 1991 with NTT+SUSI under better seeing conditions. More recently, R 127 has been observed using WFPC2 on *HST* (archive data, GO 6540, P.I. Schulte-Ladbeck). Again, stars #8 and #10 are visible, as well as several fainter spots, but the combination of the diffraction pattern, saturation by star #7, and the presence of nebulosity makes these spots difficult to identify.

R 128 is resolved into at least 33 stars. It is therefore more populated than its neighboring cluster R 127. The main component, #37 with $y = 10.82$ mag, should be considered as the star usually referred to as R 128, since the next brightest star of the cluster, #24 with $y = 13.16$ mag, is much weaker.

Figure 8 shows the color-magnitude ($C-M$) diagrams of the R 127 and R 128 clusters. The position of the brightest star of

Table 1. Photometry of the R 127 components.

Star	α (2000.0)	δ (2000.0)	Strömgren y (mag)	$(b - y)$ (mag)	M_V (mag)	Spectral type	Notes
1	5:36:42.8	-69:29:58.3	17.75	-0.08			
2	5:36:43.0	-69:29:56.4	15.91	-0.08			
3	5:36:43.2	-69:29:45.6	12.12	0.02	-7.27	B0 Ia (N wk)	Fig. 7
4	5:36:43.4	-69:29:56.0	16.12	0.01			
5	5:36:43.5	-69:29:54.7	15.03	-0.04			
6	5:36:43.6	-69:29:51.5	16.78	0.10			
7	5:36:43.7	-69:29:47.4	9.37	0.23	-10.39	Peculiar A supergiant	Fig. 3. The LBV object R 127
8	5:36:43.8	-69:29:46.2	14.39	0.35			
9	5:36:43.9	-69:29:51.3	15.78	0.24			
10	5:36:44.0	-69:29:44.5	17.15	0.13			
11	5:36:44.6	-69:29:49.6	15.81	0.02			
12	5:36:44.6	-69:29:52.2	17.37	-0.11			
13	5:36:44.6	-69:29:46.0	-	-			
14	5:36:44.8	-69:29:57.3	18.87	-			

Table 2. Photometry of the R 128 components.

Star	α (2000.0)	δ (2000.0)	Strömgren y (mag)	$(b - y)$ (mag)	M_V (mag)	Spectral type	Notes
15	5:36:45.7	-69:29:55.5	16.92	0.29			
16	5:36:45.9	-69:29:58.9	14.94	0.02	-4.45	O9.7 II	Fig. 6
17	5:36:45.9	-69:30:00.7	18.09	0.00			
18	5:36:46.3	-69:30:00.2	18.07	-			
19	5:36:46.3	-69:29:52.8	18.17	0.16			
20	5:36:46.3	-69:29:56.7	16.30	-0.02			
21	5:36:46.4	-69:30:02.6	17.22	-0.21			
22	5:36:46.5	-69:30:01.1	14.63	-0.02	-4.58	O9 III	Fig. 5
23	5:36:46.5	-69:30:04.4	15.50	-0.03	-3.66	O9 Ib	Fig. 5
24	5:36:46.5	-69:29:56.1	13.16	-0.04	-5.95	O8.5 II	Fig. 4
25	5:36:46.5	-69:29:58.3	16.50	0.00			
26	5:36:46.5	-69:30:02.8	15.29	-0.03	-3.87	O9.7 II	Fig. 6
27	5:36:46.5	-69:29:51.8	17.12	0.28			
28	5:36:46.7	-69:29:59.8	14.59	-0.04	-4.52	O9.5 III	Fig. 6
29	5:36:46.7	-69:30:01.3	18.14	0.22			
30	5:36:46.8	-69:30:04.4	17.33	0.06			
31	5:36:46.8	-69:29:58.9	16.99	0.10			
32	5:36:46.9	-69:29:57.7	15.67	-0.06	-3.35	O9.5 III	Fig. 6
33	5:36:47.0	-69:30:00.2	15.82	0.05			
34	5:36:47.0	-69:29:49.1	17.37	0.23			
35	5:36:47.1	-69:29:59.3	15.46	-0.04	-3.65	B0 III	Fig. 7. Possible contamination with #33
36	5:36:47.1	-69:29:56.3	17.47	0.30			
37	5:36:47.2	-69:29:52.2	10.82	0.05	-8.71	B1.5 Ia (N wk)	Fig. 7. The "true" R 128
38	5:36:47.2	-69:30:03.9	19.09	-			
39	5:36:47.4	-69:29:58.0	15.67	-0.01	-3.58	B0 III	Fig. 7
40	5:36:47.4	-69:30:01.0	19.11	-			
41	5:36:47.4	-69:29:59.7	19.09	-			
42	5:36:47.7	-69:29:58.4	17.72	-0.03			
43	5:36:47.7	-69:29:51.8	15.83	-0.07			
44	5:36:47.9	-69:29:59.7	18.41	-0.05			
45	5:36:48.0	-69:29:56.0	13.37	-0.05	-5.70	O9 II	Fig. 5
46	5:36:48.1	-69:29:51.3	16.37	0.01			
47	5:36:48.2	-69:29:53.6	16.36	-0.07			

Table 3. Photometry of the brightest field stars.

Star	α (2000.0)	δ (2000.0)	Strömgren y (mag)	$(b - y)$ (mag)	M_V (mag)	Spectral types	Notes
61	5:36:37.1	-69:29:18.4	11.94	-0.08	-6.99	O7 Iaf	Fig. 4. Sk-69° 217. Apparent weak emission line redward of H-delta is an artifact
65	5:36:37.8	-69:30:16.7	15.90	-0.05			
67	5:36:37.7	-69:29:13.0	15.51	-0.03			
69	5:36:37.8	-69:29:40.8	15.03	-0.04			
70	5:36:37.8	-69:29:33.2	11.92	-0.03	-7.24	O8 Iab(f)	Fig. 4. Sk-69° 218. Apparent weak emission line near He II λ 4686 is blueward of that wavelength
97	5:36:39.9	-69:30:07.3	15.86	0.90			
100	5:36:40.0	-69:29:31.6	14.76	0.01			
109	5:36:40.6	-69:30:09.9	15.53	0.53			
112	5:36:40.8	-69:29:29.8	15.82	-0.05			
113	5:36:40.8	-69:29:53.1	14.00	0.00	-5.30	O9.7 II	Fig. 6
159	5:36:43.9	-69:29:09.8	15.81	-0.08			
160	5:36:43.9	-69:30:02.3	15.88	-0.08			
161	5:36:44.0	-69:29:26.8	15.84	0.37			
162	5:36:44.1	-69:30:05.1	15.45	-0.10			
211	5:36:46.8	-69:29:13.9	15.41	-0.09			
217	5:36:47.2	-69:30:29.0	15.26	-0.03			
219	5:36:47.4	-69:30:27.1	14.63	-0.08			
222	5:36:47.5	-69:30:09.4	15.58	-0.10			
249	5:36:49.3	-69:29:30.8	15.37	-0.11			
265	5:36:50.6	-69:29:57.4	15.64	0.07			
268	5:36:50.8	-69:30:16.7	15.52	0.08			
281	5:36:56.8	-69:29:27.3	15.15	-0.31		O9.7:	Fig. 6. He II λ 4686 absorption is weak indicating high luminosity, but Si IV is also weak indicating the opposite. This discrepancy is likely due to noise rather than a real peculiarity.
283	5:36:34.3	-69:30:41.0	-	-		B0 III	Fig. 7
284	5:36:31.0	-69:30:53	-	-		B1.5	Fig. 7
285	5:36:51.8	-69:30:24.3	14.03	-			
286	5:36:52.6	-69:30:22.8	15.30	-			
287	5:36:53.2	-69:29:04.9	14.72	-			
288	5:36:53.2	-69:28:40.8	14.51	-			
289	5:36:53.8	-69:30:23.0	14.83	-			
290	5:36:54.2	-69:28:58.2	13.61	-			
291	5:36:54.3	-69:28:43.6	15.76	-			

the sample, #7 ($y = 9.37$, $(b - y) = 0.23$ mag), is confirmed by independent photometric results. In fact the light curve of R 127 from 1985 to 2002 (Stahl, private communication) shows that the LBV attained a brightness of $V = 9.35 \pm 0.2$ at the end of the year 1997. Similarly, the correlation between the magnitude and color of R 127 (Spoon et al. 1994) indicates a color of $(b - y) = 0.23 \pm 0.05$ mag corresponding to a visual brightness of $y = 9.36$ mag.

The C-M diagram shows a main sequence centered on $(b - y) \sim 0.00$ mag for both clusters. The intrinsic colors of the O type stars vary from -0.12 to -0.15 mag for T_{eff} ranging from 30 000 to 50 000 degrees and $\log g = 3.50$ to 5.00 (Relyea & Kurucz 1978). Taking $(b - y)_0 = -0.14$ mag as the average value and using the conversion relation

$E(b - y) = 0.67E(B - V) + 0.02$ (Kaltcheva & Georgiev 1992), we find $E(B - V) = 0.18$ mag ($A_V = 0.6$ mag) for the average reddening of clusters R 127/R 128. The reddest components of the R 127 cluster are #8 and #9, which we will discuss in Sect. 5. The R 128 cluster also shows a number of red stars.

The absolute magnitudes, M_V , listed in Tables 1–3 were derived assuming equality between the Strömgren y and Johnson V magnitudes. Taking a distance modulus of 18.6 mag for the LMC (Whitelock et al. 1997), we used the above-mentioned relation to correct for the reddening of each star. The corresponding luminosities used in Sect. 5 were obtained from the bolometric corrections given by Vacca et al. (1996) for O type stars. There is now general agreement that Vacca et al. (1996) overestimate the temperatures and luminosities

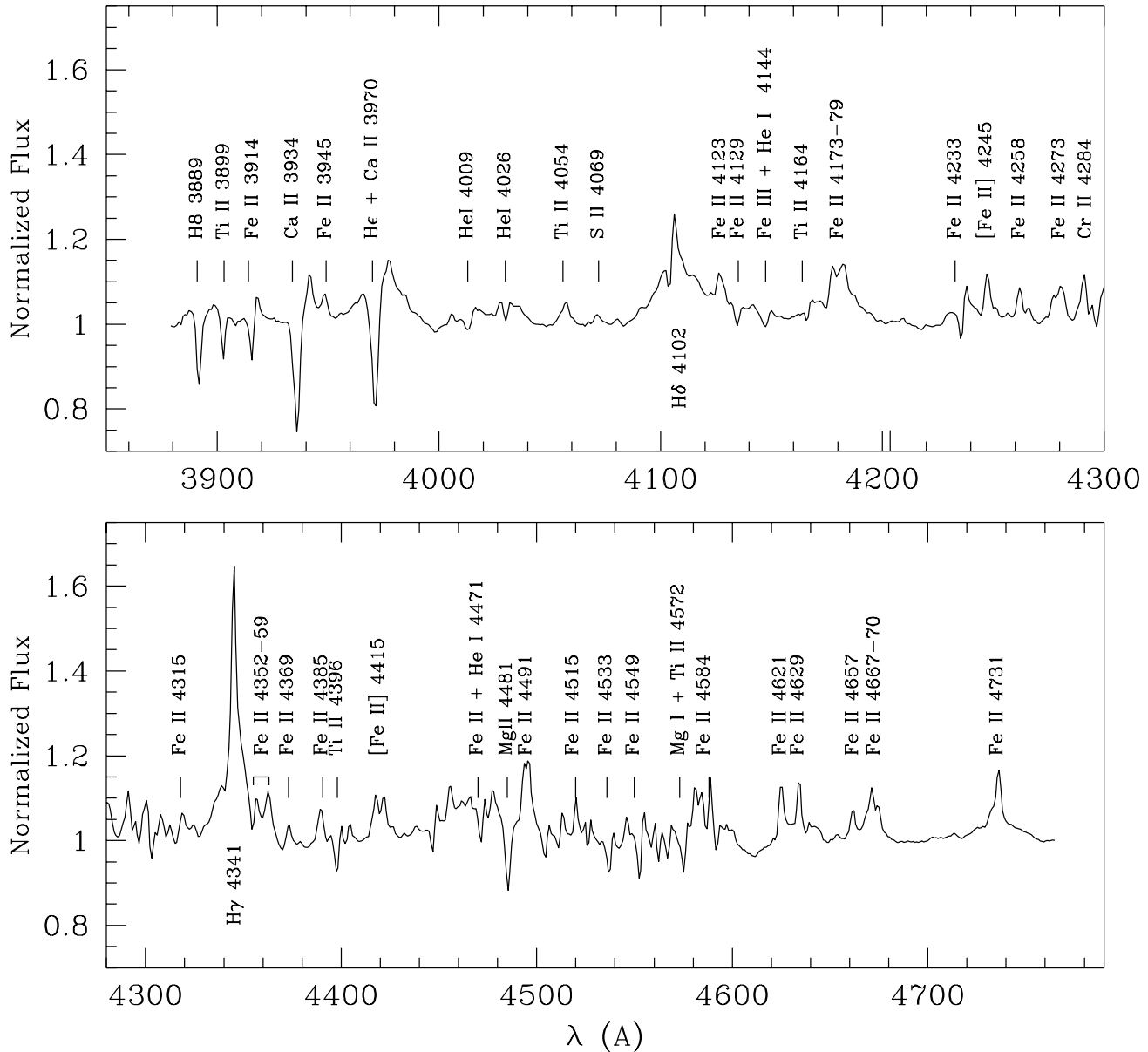


Fig. 3. A spectrum of R 127 obtained in 1997 November using the ESO NTT+EMMI with grating #12.

(Martins et al. 2002). However, their calibration is adequate for our purpose in this paper, especially since we use their bolometric corrections. For B types and the LBV R 127, which shows a (peculiar) A type supergiant spectrum, we used the calibration by Fitzpatrick & Garmany (1990).

3.2. Field stars

Photometry was obtained for 244 field stars lying in the direction of the R 127 and R 128 clusters. Among them those brighter than $y = 16$ mag are listed in Table 3. Stars #283 and #284, situated out of our images, appear in this table because they happened to fall on the spectrograph slit and therefore have spectral classifications. The brightest stars of this sample are #61, #70 (more commonly known as Sk $-69^{\circ}217$ and Sk $-69^{\circ}218$) and then #290 and #113. The C–M diagram

for the whole sample of the field stars is displayed in Fig. 8, and their detailed photometry is available upon request.

4. Spectral types

The spectral classification of the OB stars was performed with respect to the digital atlas of Walborn & Fitzpatrick (1990). No classification standards with the current observational setup were available, so there may be a slightly greater uncertainty in the (lower) luminosity classes than is usual in this work, but it does not exceed one class and may well be smaller.

4.1. R 127 cluster

Spectrograms of the two brightest stars, #3 and #7, are available. These are the “preceding” (western) and “following” (eastern) components of R127 (HDE 269858), respectively, as

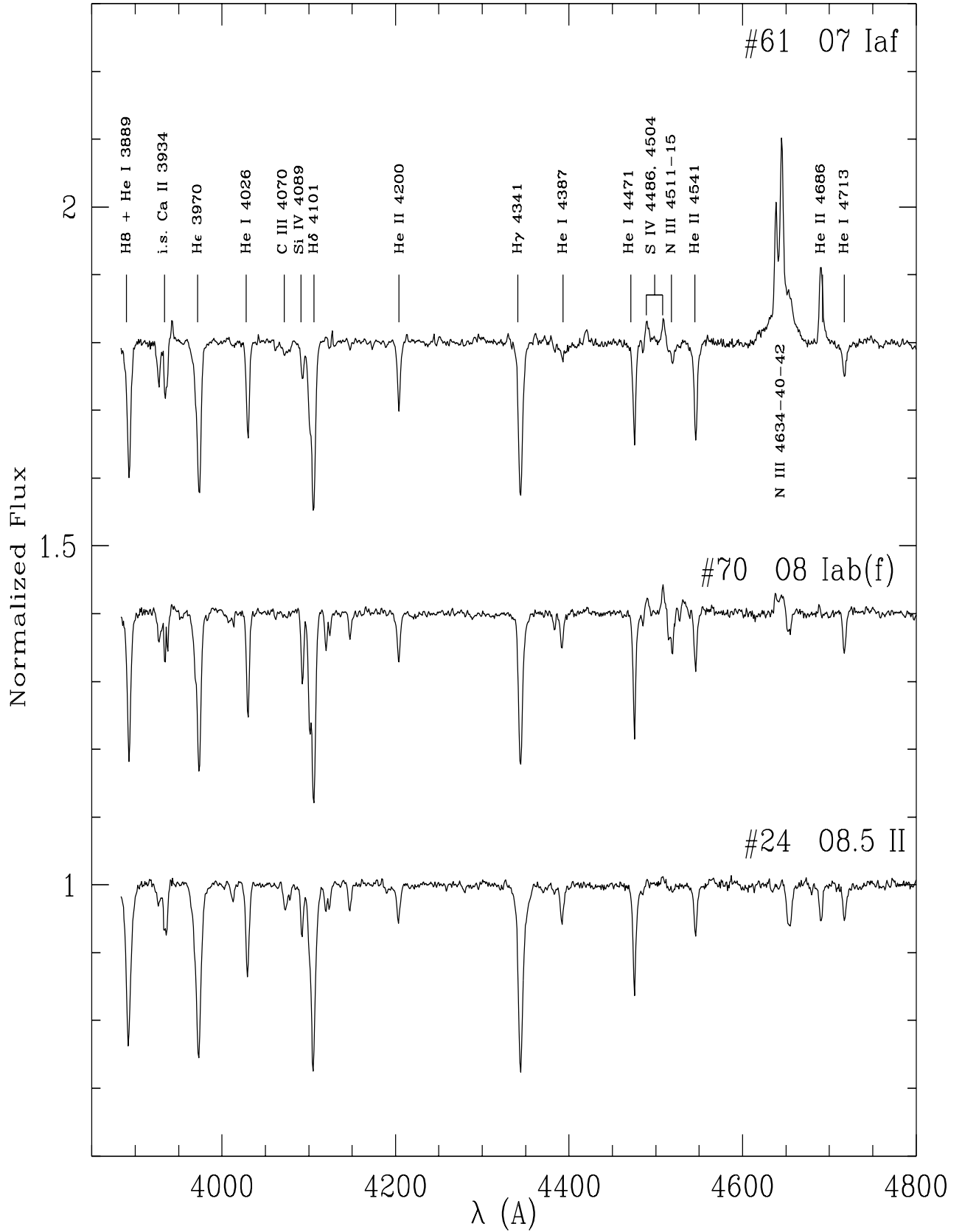


Fig. 4. Spectra of the earliest type stars towards R 127 and R 128 clusters.

denoted by Feast et al. (1960), and we confirm that the eastern component, #7, is the peculiar star. The two components

had similar apparent magnitudes when observed by Feast et al. (1960), but as discussed in the Introduction, #7 is currently in

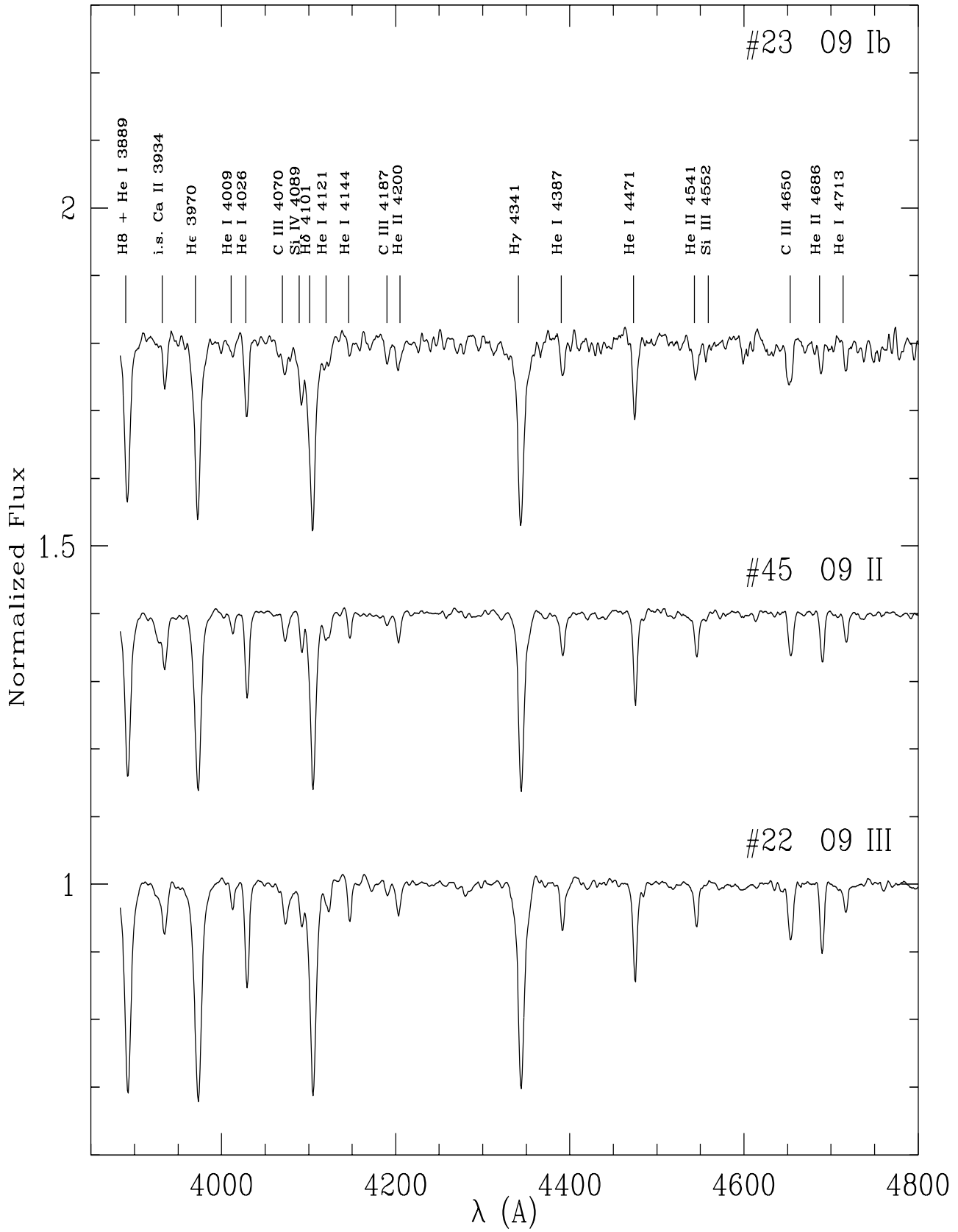


Fig. 5. Spectra of O9 type stars observed towards R 127 and R 128 clusters.

an extended LBV phase and is much brighter. Our observation of its spectrum is illustrated in Fig. 3. It is representative

of the peculiar A supergiant LBV maximum phase, dominated by emission lines of hydrogen and singly ionized heavy metals

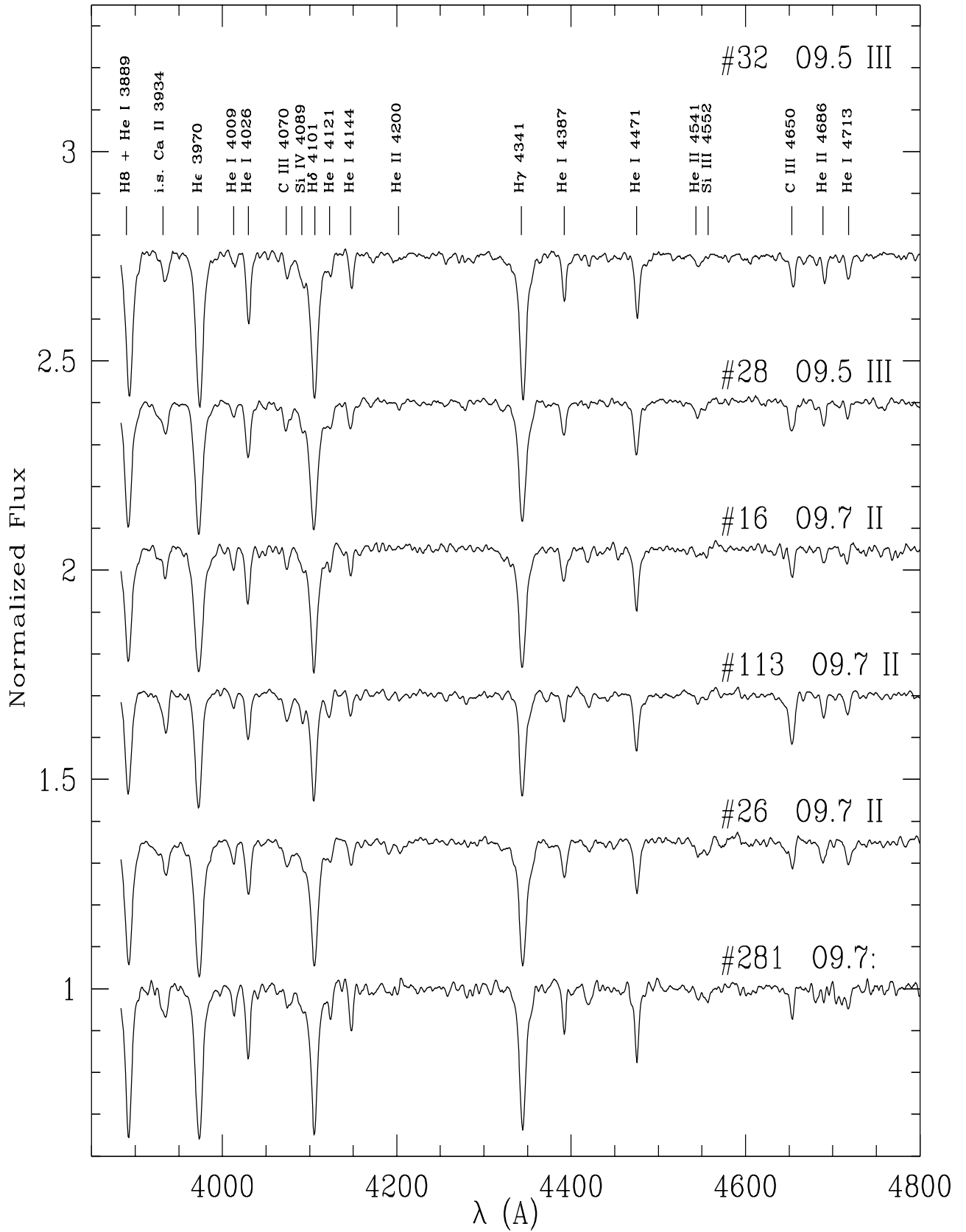


Fig. 6. Spectra of the latest O type stars observed towards R 127 and R 128 clusters.

(e.g., Fe II, [Fe II], Ti II, Cr II); see Wolf et al. (1988) for a detailed presentation of this kind of spectrum at high resolution.

We believe that our spectrogram of star #3 (Fig. 7) is the first spatially resolved observation of its spectrum. It has an

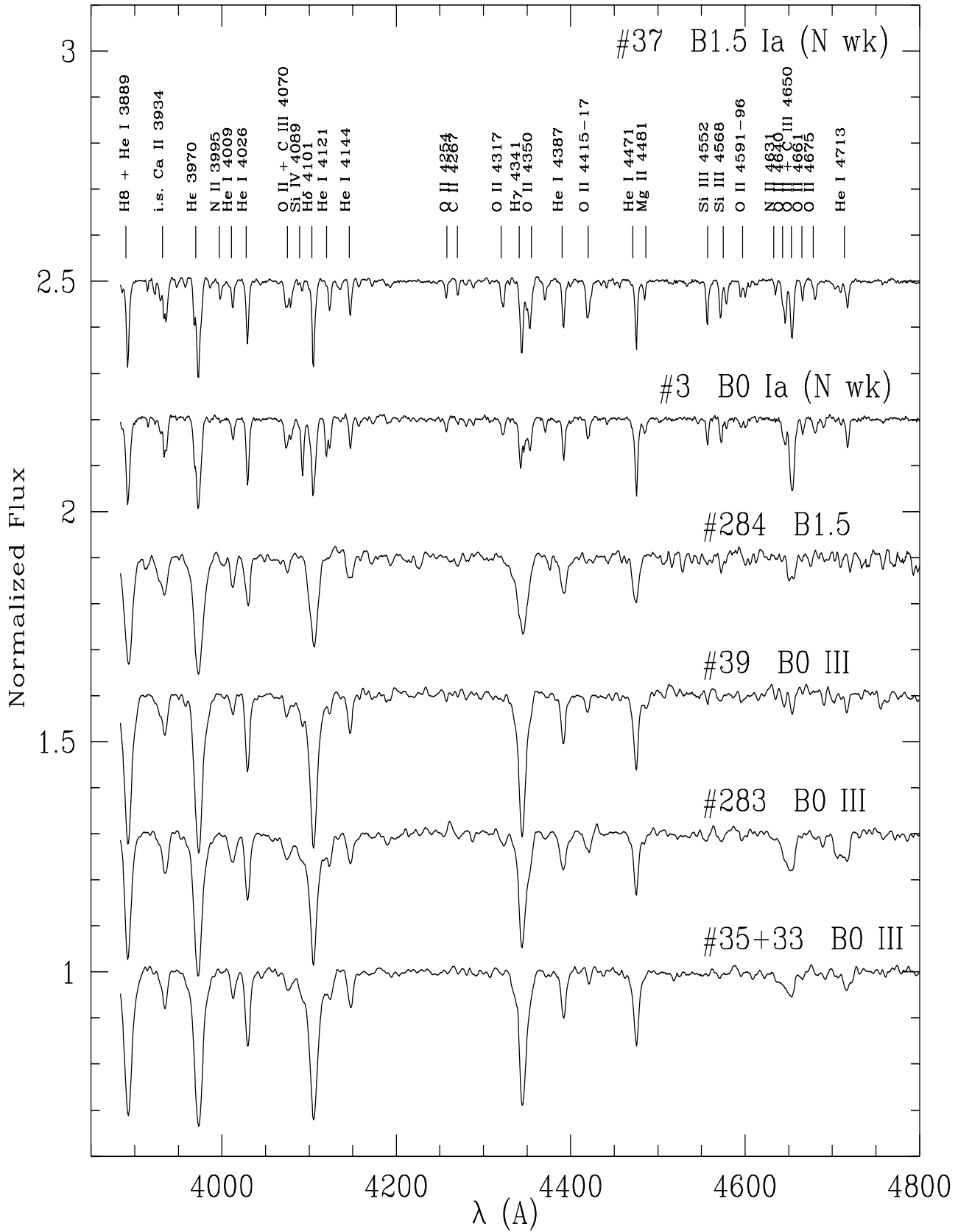


Fig. 7. B type stars observed towards R 127 and R 128 clusters.

interesting, very well defined B0 Ia type with deficient nitrogen (cf., e.g., the extreme weakness of the $\lambda 4097$ absorption in the

blue wing of H δ , which is near maximum strength in a normal spectrum of this type). The latter characteristic indicates that

this star either is a relatively un-evolved supergiant, or was a slow rotator on the main sequence (e.g., Walborn et al. 2000 and references therein).

4.2. R 128 cluster

We have spectroscopy for 11 stars in this compact cluster, which is shown in Figs. 4–7. Most of them are late-O or early-B giants (i.e., the main sequence was not reached spectroscopically), but one (#23, Fig. 5) is classified O9 Ib, and #37 is R 128 itself, the brightest star in the cluster, which we classify B1.5 Ia (N weak). R 128 was classified B1 Ia by Fitzpatrick (1988) and B2 Ia (N weak) by Fitzpatrick (1991). We prefer the intermediate type on the basis of the strength of Si iv λ 4089 and concur on the anomalous deficiency of nitrogen; e.g., N II λ 3995 reaches its maximum strength at B2 Ia and would be comparable to He I λ 4026 in a normal spectrum. Current explanations of such anomalies are as cited above for star #3 in the R 127 cluster.

4.3. Field stars

Finally, 6 stars in the surrounding field were also observed spectroscopically. The most interesting are the relatively bright stars #61 (Sk $-69^{\circ}217$) and #70 (Sk $-69^{\circ}218$) shown in Fig. 4. The Of nature of Sk $-69^{\circ}217$ was discovered by Walborn et al. (1991) and the spectral classification of O7 Iaf from the present, higher quality material is in perfect agreement with the earlier result; this is the hottest star in the present sample. On the other hand, the earlier classification of ON9 Ib for Sk $-69^{\circ}218$ is here revised to O8 Iab(f), with no nitrogen/carbon anomaly. This discrepancy can be understood in terms of the lower quality of the earlier spectrogram, which led to a later type at which the N/C line strengths would be anomalous, but they are not at the earlier type derived here. The recently identified S IV λ 4486, 4504 emission lines (Werner & Rauch 2001) are prominent in both of these spectra.

5. Discussion

The brightest members of the R 127/R 128 clusters are massive evolved stars as indicated by their spectral types. There are, however, stars residing still on the main sequence (Fig. 8), but they have been missed in our spectroscopy due to their relatively low brightness. In order to look into the evolutionary states of the clusters' stars, we have used the theoretical models of Meynet et al. (1994) for a metallicity of $z = 0.004$ and high mass loss rates. Figure 9 presents the relevant isochrones and evolutionary tracks on which are overlaid the stellar positions. The filled dots are based on the physical parameters given by Vacca et al. (1996)'s calibration for the derived spectral types. The crosses indicate the corresponding luminosities obtained from our photometry. We see that for a number of stars the observed luminosities are much smaller than those predicted by Vacca et al. (1996)'s calibration. We will briefly discuss this problem below.

The positions of the filled dots suggest that the hottest stars of the sample, #61 and #70, are ~ 3 Myr old, and have evolved

from initial masses of $\sim 80 M_{\odot}$ into late-type O supergiants. Likewise, the oldest stars, #39 and #35, are B0 supergiants with an age of ~ 6 Myr and a ZAMS mass of $\sim 25 M_{\odot}$. It seems therefore that in the R 127/R 128 region, lower mass stars formed prior to massive ones. Moreover, the positions of the crosses, taken at face value, suggest masses as low as $\sim 15 M_{\odot}$ with ages up to ~ 8 Myr.

The LBV member of the sample, star #7, does not appear in the H–R diagram since its relatively low effective temperature puts it outside the plot. It is well-known that LBV stars change their spectral type, temperature and radius, becoming cooler and larger during the visual maximum phase. However, their luminosity remains approximately constant, with $\log L/L_{\odot} = 6.1$ for R 127, as reported by several workers (Stahl et al. 1983; Wolf 1989; Lamers et al. 1998; van Genderen 2001). An effective temperature of $\log T_{\text{eff}} = 3.954$ is calculated by Lamers et al. (1998) for R 127 corresponding to its phase of visual maximum.

Star #7 is the most evolved member of the R 127/R 128 clusters, presumably because it was the most massive star of the group. An initial mass of $\sim 85 M_{\odot}$ can be attributed to the LBV progenitor from Fig. 9. A present mass of $46_{-3}^{+17} M_{\odot}$ is derived for the LBV by Lamers et al. (1998). This means that star #7 has lost $\sim 45\%$ of its mass since its formation ~ 3 Myr ago, corresponding to a constant mass loss rate of $\dot{M} = 1.3 \times 10^{-5} M_{\odot} \text{ yr}^{-1}$. However, mass loss is not a regular process and LBVs undergo drastic episodes during which they lose mass dramatically. For example, model calculations by Langer et al. (1994) show that during the first 1.5 Myr of life of a $60 M_{\odot}$ star the mass loss rate is constant, $\sim 5 \times 10^{-6} M_{\odot} \text{ yr}^{-1}$. Then it becomes much stronger, $\sim 3 \times 10^{-5} M_{\odot} \text{ yr}^{-1}$, during the next 2 Myr. The peak of mass loss during the LBV phase reaches $\sim 3 \times 10^{-3} M_{\odot} \text{ yr}^{-1}$ when the star has an age of ~ 3.4 Myr. On the other hand, association in a close binary system has been suggested for accelerating the evolution of massive stars and creating the LBV phenomenon (Tutukov & Yungelson 1980; Gallagher 1989; Humphreys & Davidson 1994). However, so far no observational support exists for this LBV being a binary system.

Figure 9 shows a discrepancy between the luminosities suggested by the spectral type calibration schemes (Vacca et al. 1996) and those derived from the photometry. While the smaller deviations, like those of stars #61, #70, #3, #45, etc., can be attributed to measurement uncertainties, a discrepancy as large as that for star #23 called for verification. This trend was first interpreted as due to a sort of bias. However, despite our efforts, no systematic errors were found in our photometry. In fact, our examination of several published papers on other regions showed that ΔM_V (the difference between the absolute magnitudes derived from spectral types and those from photometry) increases with magnitude, although with different extents (Fitzpatrick 1988; Walborn & Blades 1997; Walborn et al. 1999; Parker et al. 1992; Massey & Johnson 1993). Such trends are expected from the defining relations, if there are dispersions in the actual absolute magnitudes or distances, or systematic effects in the spectral classification, absolute-magnitude calibration, or photometry. Uncorrected differential

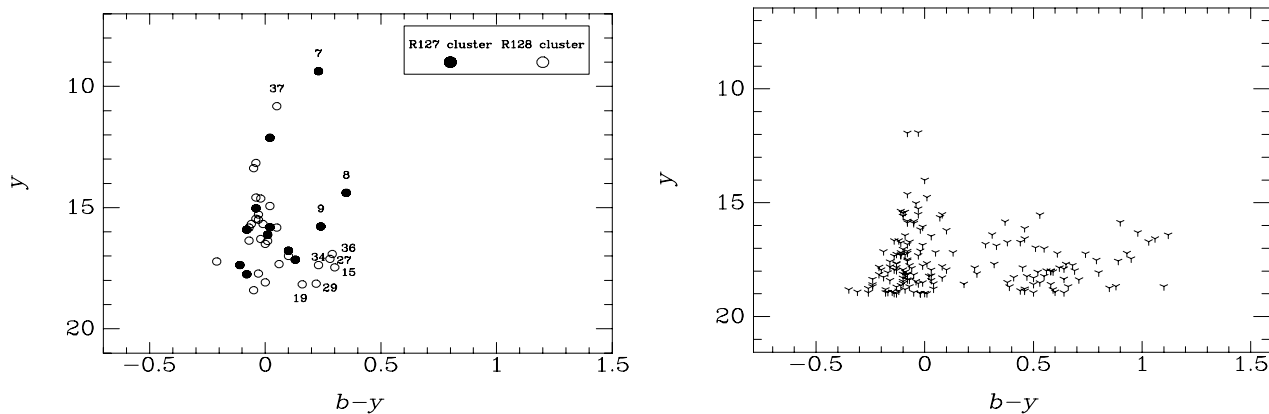


Fig. 8. Color-magnitude diagram of stars in R 127 and R 128 clusters (left panel). Diagram for the field stars around R 127 and R 128 clusters (right panel).

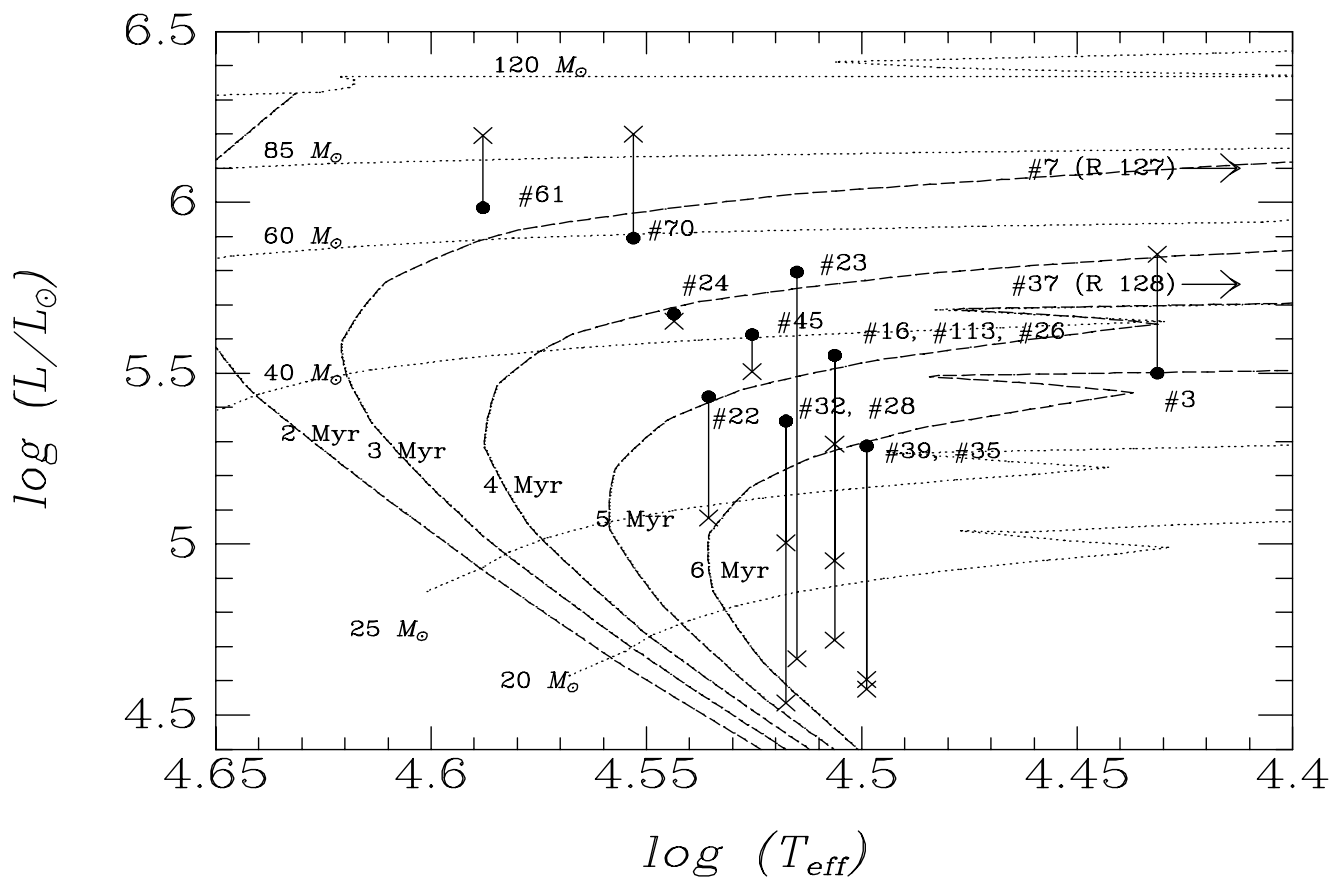


Fig. 9. Theoretical H-R diagram (Meynet et al. 1994) for classified stars in the LMC clusters R 127 and R 128. The dashed lines indicate isochrones with ages 2 to 6 Myr and the dotted lines the evolutionary tracks for masses 20 to $120 M_{\odot}$. Filled circles represent the stars for which spectral classification is available. The positions are based on the calibration derived by Vacca et al. (1996) for O and early B stars and that by Fitzpatrick & Garmany (1990) for later types. The crosses represent the luminosities calculated using the photometric results of this paper.

extinction or relative errors in the calibration will broaden the distribution about the trends.

Aperture photometry observations previously performed on R 127 used diaphragms of $10''$ to $15''$ in diameter. As a result, the global magnitude of a small group of stars was mistaken for that of a single source. Assuming that we can simulate such a measurement by co-adding the stars found inside a circle of $10''$ centered on star #7 (which are stars #8, #3, #10,

#9 and #6), we find that the measured y magnitude would be 9.27 instead of 9.37. This small difference shows that the contribution of the weak companions identified in this work is not significant for the luminosity of the main object.

As for the brightest member of the R 128 cluster, star #37, it is a supergiant B1.5 Ia (N wk) with $\log L/L_{\odot} = 5.76$ and $\log T_{\text{eff}} = 4.24$ (van Genderen 2001) and therefore lies outside our H-R diagram (Fig. 9). This star is known to be variable

and has even previously been dubbed as an LBV candidate (van Genderen 2001). Indeed an initial mass of $\sim 50 M_{\odot}$, as derived from Fig. 9, does not rule out the possibility for star #37 to become an LBV (Maeder 1997; Langer et al. 1994).

As mentioned in Sect. 3.1, some of the cluster components show rather red colors. In particular, star #8, the closest neighbor of the LBV, lying $1''.5$ away, has the reddest color. This reminds one of the LMC transition star R 84 which has a close evolved component of type M2 Ia lying $\sim 1''.7$ from it (Heydari-Malayeri et al. 1997). Note, however, that R 84 is a lower mass object belonging to a B-type cluster. Anyhow, presently we cannot determine whether star #8 is evolved, and the red color of this star may have a totally different origin. We are aware of the color accuracies involved (Sect. 3.1), nevertheless if star #8 is physically associated with the cluster, and not a sight-line coincidence, its color could be due to contamination by the ejecta from the LBV. Clampin et al. (1993) measure a size of $8''.0 \times 9''.0$ (1.9×2.2 pc) for the circumstellar nebula lying at a position angle of 165° . Even a smaller nebula, as found by Stahl (1987), with a size of $3''.2 \times 4''.4$ (0.8×1.1 pc), can affect the color measurements of star #8. A larger nebula would also explain the red color of star #9.

6. Concluding remarks

The decomposition of the LMC compact star clusters R 127 and R 128 into at least 14 and 33 components respectively and medium-dispersion spectroscopy carried out in very good seeing conditions have allowed us to study the stellar contents of these interesting objects. This work is essential since the R 127 cluster harbors the most prominent LBV object in the LMC. We resolve the core of R 127 into four components and clearly identify the LBV object, which shows spectral features typical of a visual maximum phase. Moreover, we present the first spatially resolved spectrum of the brightest neighbor of the LBV, star #3 lying at a separation of $3''.3$. It turns out to be a supergiant B0 Ia (N wk).

We also show that the star currently known as R 128 is in fact the component number #37 of an adjacent cluster. A good quality spectrum of this supergiant leads to a revised classification of B1.5 Ia (N wk).

The two clusters are composed of evolved massive stars. The oldest members are ~ 6 – 8 Myr old and the most massive one has an initial ZAMS mass of $\sim 80 M_{\odot}$. These age estimates are in agreement with the fact that no H II regions are associated with the clusters. The most massive stars have had enough time to disrupt the molecular cloud and the nebula, and the earliest spectral types are no longer present.

This spectroscopic study misses the main sequence stars of the clusters, which probably have lower initial masses with respect to the evolved ones. It will therefore be interesting to observe them spectroscopically in order to determine their real status. It will also be attractive to study the dynamics of the clusters by obtaining accurate radial velocities of the members.

Acknowledgements. We are particularly indebted to Dr. Pierre Magain, Institut d'Astrophysique et de Géophysique de l'Université de Liège, Belgium, and his group for warm hospitality offered to F.M.

while he learned to use the MCS deconvolution algorithm. Our thanks go also to Dr. Frédéric Courbin for discussions and advice at several occasions during his visits to Paris. We are also grateful to the referee, Dr. A. M. van Genderen, for his helpful comments. We would like also to thank Dr. Otmar Stahl, Landessternwarte, Heidelberg, for discussions and information about the monitoring of R 127 and Dr. Jesús Maíz-Apellániz, STScI, about the absolute-magnitude trends.

References

- Ardeberg, A., Brunet, J. P., Maurice, E., & Prevot, L. 1972, *A&AS*, 6, 249
- Clampin, M., Nota, A., Golimowski, D. A., Leitherer, C., & Durrance, S. T. 1993, *ApJ*, 410, L35
- Davies, R., Elliott, K., & Meaburn, J. 1976, *Mem. R. Astron. Soc.*, 81, 89
- Feast, M. W., Thackeray, A. D., & Wesselink, A. J. 1960, *MNRAS*, 121, 337
- Fitzpatrick, E. L. 1988, *ApJ*, 335, 703
- Fitzpatrick, E. L. 1991, *PASP*, 103, 1123
- Fitzpatrick, E. L., & Garmany, C. D. 1990, *ApJ*, 363, 119
- Gallagher, J. S. 1989, in *ASSL 157*, IAU Colloq. 113, *Physics of Luminous Blue Variables*, ed. K. Davidson, A. Moffat, & H. Lamers, 185
- Henize, K. G. 1956, *ApJS*, 2, 315
- Heydari-Malayeri, M., Courbin, F., Rauw, G., Esslinger, O., & Magain, P. 1997, *A&A*, 326, 143
- Humphreys, R. M., & Davidson, K. 1994, *PASP*, 106, 1025
- Isserstedt, J. 1975, *A&AS*, 19, 259
- Kaltcheva, N., & Georgiev, L. 1992, *MNRAS*, 259, 166
- Kukarkin, B., Kholopov, P., & Efremov, Y. N. 1974, *Sec. Suppl. Third Edition Gen. Cat. Var. Stars*, Nauka, Moscow, 10
- Lamers, H. J. G. L. M., Bastiaanse, M. V., Aerts, C., & Spoon, H. W. W. 1998, *A&A*, 335, 605
- Lamers, H. J. G. L. M., Nota, A., Panagia, N., Smith, L. J., & Langer, N. 2001, *ApJ*, 551, 764
- Langer, N., Hamann, W.-R., Lennon, M., et al. 1994, *A&A*, 290, 819
- Lucke, P. B., & Hodge, P. W. 1970, *AJ*, 75, 171
- Maeder, A. 1997, in *ASP Conf. Ser.*, ed. A. Nota & H. Lamers, 120, 374
- Magain, P., Courbin, F., & Sohy, S. 1998, *ApJ*, 494, 472
- Manfroid, J., Sterken, C., Bruch, A., et al. 1991, *A&AS*, 87, 481
- Manfroid, J., Sterken, C., Cunow, B., et al. 1994, *A&AS*, 109, 329
- Martins, F., Schaerer, D., & Hillier, D. J. 2002, *A&A*, 382, 999
- Massey, P., & Johnson, J. 1993, *AJ*, 105, 980
- Meynet, G., Maeder, A., Schaller, G., Schaerer, D., & Charbonnel, C. 1994, *A&AS*, 103, 97
- Nota, A., & Clampin, M. 1997, in *Luminous Blue Variables, Massive Stars in Transition*, ed. A. Nota, & H. Lamers, *ASP Conf. Ser.*, 120, 303
- Nota, A., & Lamers, H. 1997, in *ASP Conf. Ser.*, ed. A. Nota, & H. Lamers, 120
- Nota, A., Leitherer, C., Clampin, M., & Gilmozzi, R. 1991, in *Wolf-Rayet Stars and Interrelations with Other Massive Stars in Galaxies*, ed. K. van der Hucht, & B. Hidayat, *IAU Symp.*, 143, 561
- Parker, J. W. 1997, in *Luminous Blue Variables: Massive Stars in Transition*, ed. A. Nota, & H. Lamers, *ASP Conf. Ser.*, 120, 368
- Parker, J. W., Garmany, C. D., Massey, P., & Walborn, N. R. 1992, *AJ*, 103, 1205
- Relyea, L. J., & Kurucz, R. L. 1978, *ApJS*, 37, 45

- Sanduleak, N. 1970, *Cerro Tololo Inter-American Obs. Cont.*, 89
- Schulte-Ladbeck, R. E., Leitherer, C., Clayton, G. C., et al. 1993, *ApJ*, 407, 723
- Shannon, C. 1949, *Proc. I. R. E.*, 37, 10
- Smith, L. J., Nota, A., Pasquali, A., et al. 1998, *ApJ*, 503, 278
- Spoon, H. W. W., de Koter, A., Sterken, C., Lamers, H. J. G. L. M., & Stahl, O. 1994, *A&AS*, 106, 141
- St-Louis, N., Turbide, L., & Moffat, A. 1997, in *Luminous Blue Variables: Massive Stars in Transition*, ed. A. Nota, & H. Lamers, *ASP Conf. Ser.*, 120, 187
- Stahl, O. 1987, *A&A*, 182, 229
- Stahl, O., Leitherer, C., Wolf, B., & Zickgraf, F.-J. 1984, *A&A*, 131, L5
- Stahl, O., Wolf, B., Klare, G., et al. 1983, *A&A*, 127, 49
- Sterken, C. 1983, *The Messenger*, 33, 10
- Sterken, C., Manfroid, J., Anton, K., et al. 1993, *A&AS*, 102, 79
- Sterken, C., Manfroid, J., Beele, D., et al. 1995, *A&AS*, 113, 31
- Tutukov, A. V., & Yungelson, L. R. 1980, *Soviet Astron. Lett.*, 6, 271
- Vacca, W. D., Garmany, C. D., & Shull, J. M. 1996, *ApJ*, 460, 914
- van Genderen, A. M. 2001, *A&A*, 366, 508
- van Genderen, A. M., de Groot, M., & Sterken, C. 1997, *A&AS*, 124, 517
- van Genderen, A. M., Sterken, C., de Groot, M., & Reijns, R. A. 1998, *A&A*, 332, 857
- Walborn, N. R. 1977, *ApJ*, 215, 53
- Walborn, N. R. 1982, *ApJ*, 256, 452
- Walborn, N. R., & Blades, J. C. 1997, *ApJS*, 112, 457
- Walborn, N. R., Drissen, L., Parker, J. W., et al. 1999, *AJ*, 118, 1684
- Walborn, N. R., Evans, I. N., Fitzpatrick, E. L., & Phillips, M. M. 1991, in *Wolf-Rayet Stars and Interrelations with Other Massive Stars in Galaxies*, ed. K. van der Hucht, & B. Hidayat, *IAU Symp.*, 143, 505
- Walborn, N. R., & Fitzpatrick, E. L. 1990, *PASP*, 102, 379
- Walborn, N. R., Lennon, D. J., Heap, S. R., et al. 2000, *PASP*, 112, 1243
- Werner, K., & Rauch, T. 2001, in *Eta Carinae and Other Mysterious Stars: The Hidden Opportunities of Emission Spectroscopy*, ed. T. Gull, S. Johannson, & K. Davidson, *ASP Conf. Ser.*, 242, 229
- Whitelock, P. A., van Leeuwen, F., & Feast, M. W. 1997, in *ESA SP-402: Hipparcos – Venice '97*, 402, 213
- Wolf, B. 1989, *A&A*, 217, 87
- Wolf, B., Stahl, O., Smolinski, J., & Casatella, A. 1988, *A&AS*, 74, 239